HYDRODYNAMICS AND TRANSPORT IN THE COASTAL ZONE OF SÃO PAULO – BRAZIL

PAULO C. LEITÃO

Hidromod Lda, Av. Manuel da Maia, 36, 3º es
100-201 Lisboa, Portugal

JOSÉ C. LEITÃO

Hidromod Lda, Av. Manuel da Maia, 36, 3º es
100-201 Lisboa, Portugal

RAMIRO NEVES

Instituto Superior Técnico, Pavilhão de Mecânica
1049-001 Lisboa, Portugal

GILBERTO BERZIN

Universidade Santa Cecília, Rua Oswaldo Cruz, 266 - Boqueirão
11045-907 Santos/SP, Brazil

ADÉLIO J. R. SILVA

Hidromod Lda, Av. Manuel da Maia, 36, 3º es
100-201 Lisboa, Portugal

The port activities in the area of Santos (São Paulo, Brazil), imply systematic works of dredging and disposal of sediments. The dredged material is discharged in the coastal zone. Hydrodynamics, deposition and remobilization of fine sediments processes were reproduced using a hydrodynamic model coupled with a lagrangian fine sediment transport model. This paper addresses the subjects of: i) hydrodynamic forcing in the coastal zone of São Paulo, ii) nested modeling, boundary conditions and model forcing, iii) fine sediment transport mechanisms. The main hydrodynamic forcing mechanisms were identified: local wind, sub-inertial oscillations forced by large scale atmospheric processes and tide. A special reference is made to the sub-inertial oscillations that can be easily identified in the tidal Gauges and ADCP data. The hydrodynamic model was validated with ADCP and tidal gauge data. The numerical tool implemented was used to identify the area of influence of resuspended sediments from several disposal areas for dredged material.

1. Introduction

Due to the highly nonlinear relation between currents and sediment transport, it is necessary to have a clear notion of the spatial and temporal variability of the hydrodynamics. Numerical modeling associated with field data seems to be an

efficient way to achieve this goal. The hydrodynamic processes in coastal areas, when compared with more enclose domains like estuaries, are more difficult to simulate. In one hand, coastal areas are less dissipative because depths are greater and velocities are lower. On the other hand, there is an overlapping of several processes with very different spatial and time scales like tide, upwelling jet, coastal trapped waves and large scale currents. The first characteristic requires a special care in controlling numerical diffusion, especially in the presence of processes associated with density fronts (Tartinville et al. 1998). The overlapping of processes with different scales is also a challenge from the numerical point of view. This characteristic of the coastal zones raises problems especially in the definition of model open boundaries. This is presently one of the main subjects of the hydrodynamic modeling community (Marchesiello et al. 2001).

2. Study area and problem definition

The study area is located in the coastal zone of São Paulo more specifically in the Santos estuary and the adjacent coastal zone (Figure 1). The region of Santos – São Vicente Estuarine Complex (23°30'-24°S - 46°05'-46°30'W) is formed by two islands (São Vicente and Santo Amaro) very close to the continent delimiting three channels: Santos, São Vicente and Bertioga. This area is located in the Southern limit of the tropical zone with mean temperatures of 22°C, average annual precipitation of 2500 mm and is surrounded by the Serra do Mar slopes. The coastal plains were originally covered by extensive mangrove forests, which were gradually occupied by the industrial complex of Cubatão, established since 1940, by an urban area and by the Santos harbor (the most important Brazilian port).

The port activities imply systematic dredging and disposal of sediments. These activities may have a negative impact on the environment, since part of the sediments is contaminated (due to the upstream Cubatão industrial areas). Thus, the areas of influence of the sediment deposition sites have to be studied, and the sites approved by the local environmental authority prior to their use.

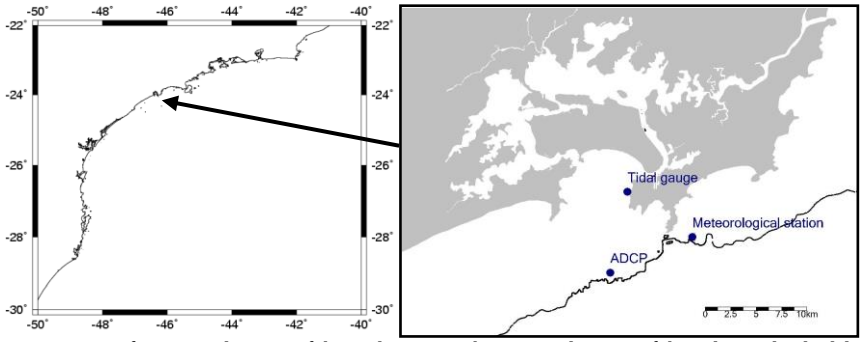

Figure 1 – Left picture – location of the study area. Right picture - location of the Palmas Island tidal gauge, the place where the ADCP was moored and the Moela Island meteorological station.

2.1. *Main hydrodynamic characteristics*

In São Paulo's coastal zone, local and remote influence of meteorological conditions is important. Tide also plays a role, mostly in the fluxes inside and outside of the estuarine areas. According to Castro and Lee (1995), continental shelf waves can be one of the mechanisms behind the sub-inertial sea level oscillations observed along the Southeast Brazilian coast. These waves are generated south of the study area due to atmospheric disturbances and propagate NE, along the Southeast Brazilian shelf. Camargo et al. (1999), based on sea level measurements along the coast, also enlightens the strong correlation between those records and the meteorological events.

Measurements of sea level, currents and local wind were obtained in summer and winter conditions in the framework of the present study. These measurements showed a strong correlation between the sub-inertial variations of the sea level and the currents in the coastal zone, at depths ranging from 15 to 25 m and distances from the coast of about 5 to 10 km. This correlation confirmed the findings of Castro and Lee (1995) and also showed that this is an important forcing mechanism of the hydrodynamics in the coast of São Paulo.

2.2. *Data analysis*

The field data available to describe the hydrodynamics in the study area was: (i) measurements made by the tidal Gauge of Palmas Island; (ii) current meter data collected by an ADCP moored in the bathymetric of 20 m in front of the Santos estuary (Figure 1).

The main hydrodynamic characteristics of the study area described earlier can be seen very clearly in the data collected during two months by the ADCP. Figure 2 represents currents intensity (colour) function of time (x) and depth (y). This result shows that the velocity profile is highly homogeneous in the

water column. In the ADCP location currents can reach velocities up to 1 m/s in the all water column and in extreme conditions. This means that in this location fine sediments are easily resuspended.

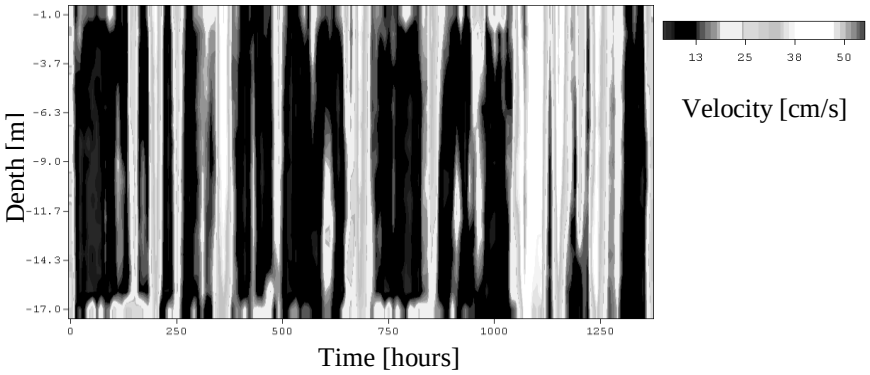

Figure 2 – Current intensity in a 2 months period. Color represents current intensity function of time (x) and depth (y).

In the spectral analysis of the velocity along shore component, averaged in depth, it is possible to identify the time scales associated with the main variability. The scale between 4 and 8 days (sub-inertial oscillations scales) are responsible for the main variability (Figure 3). The semi-diurnal and diurnal sign of tide is comparatively very low. However, for the cross shore component, the effect of tide is much clearer. This is due to the currents generated by the exchanges between the estuary and the coast. The spectral analysis of the water level shows that variability is dominated very strongly by tide.

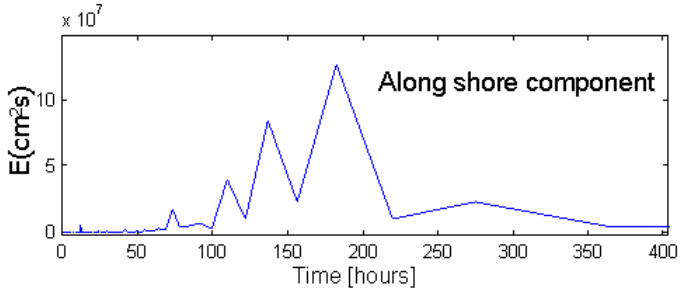

Figure 3 – Spectral analysis of the velocity along shore component averaged in depth measured by an ADCP (Figure 1).

3. Methodology

The MOHID system (http://www.mohid.com) was the numerical tool used to evaluate the risk of resuspension and transport to the shore line of the dumped

dredged material. This system was developed using an object oriented programming philosophy. The main goal of this system is to model physical and biogeochemical processes in the marine environment. The hydrodynamics and the sediment deposition and remobilization processes were reproduced using the hydrodynamic module coupled with the lagrangian fine sediment transport module.

3.1. *Hydrodynamic modeling*

The MOHID hydrodynamic module allows the overlapping of different scales (nested models) and systems (oceans and estuaries). MOHID system versatility can be easily demonstrated by a series of previous applications: in the study of oceanic circulation (Coelho et al., 2002) and also hydrodynamic (Martins et al. 2001) and sediment transport in estuaries (Cancino and Neves 1998).

The hydrodynamic module of the MOHID system generates and updates the flow information, solving the primitive equations of motion in the three-dimensional space for incompressible fluids. Hydrostatic equilibrium is assumed as well as the Boussinesq approximation. The spatial discretization of these equations is done with a finite volume technique (Martins et al., 2001) which allows the use of a system of generic vertical coordinates, making the model independent of vertical discretization. Therefore the model can be easily applied to different places with diverse geometries. The time discretization is based in a semi-implicit scheme. It was also incorporated a turbulence scheme based on GOTM (General Ocean Turbulence), which is largely validated. In this way, the model is prepared to compute the main physical forcing mechanisms such as density gradients, tide, wind, fresh water inputs and others.

Although a significant density front appears in the area occasionally (probably coming from the Rio de La Plata region) the stratification does not change significantly the homogeneity of the currents in the water column, due to the barotropic nature of the forcing mechanism (a strong pressure gradient due to tide and sub-inertial sea level oscillations).

Based on these hydrodynamic characteristics, essentially barotropic, a 2D approach was adopted. The computational efficiency is also increased with the use of only one layer in the hydrodynamic model.

3.2. *Boundary conditions*

The hydrodynamic module was implemented following a nested approach, with two different levels of domains (Figure 4).

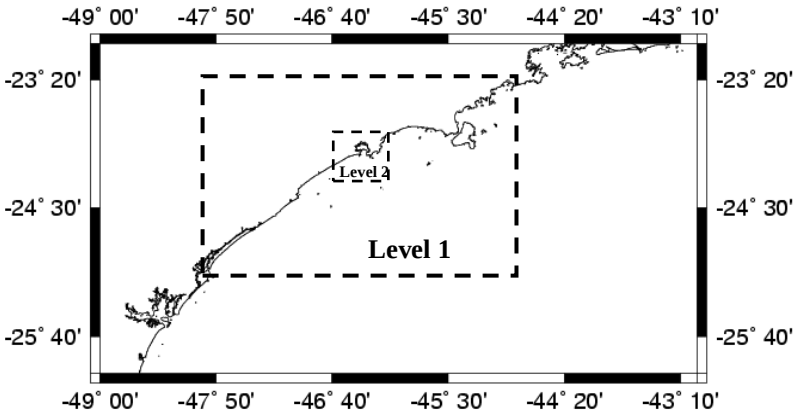

Figure 4 – The domain of each model level (level 1 and 2). In this nested approach two levels were used.

In both levels, for the land boundaries null flux of mass and momentum was imposed. The inter-tidal areas were computed using a wetting and drying methodology described in Martins et al. (2001). In the first level, and for the water levels open boundary, a radiative boundary condition, was used:

$$\frac{\partial \eta}{\partial t} + \left(\overrightarrow{c_E} \cdot \vec{n}\right)\nabla \eta = \frac{1}{T_d}\left(\eta_{ref} - \eta\right) \quad (1)$$

where η is open boundary normal vector, T_d is decay time, η_{ref} is reference water level, η is water level computed by the model, c_E is celerity of external waves.

The reference water level along the boundary was assumed equal to the global solution FES95.2 plus sub-inertial oscillations. The decay time was assumed minimum in the larger depths and off-shore (180 s) and maximum in the smaller depths and near-shore (1800 s). These values were obtained after sensitivity analysis aimed at reducing the "noise" produced by the open boundaries. As to surface boundary conditions in the water-air interface, the flux of momentum is computed from wind data measurements in the Moela Island (Figure 1).

The nested methodology used for the lower level (level 2) is one way with boundary relaxation (Oey and Chen, 1992). The spatial domain of this level model covers the study area, Santos estuary and the adjacent coastal area.

One of the main challenges of this work was the overlapping in the open boundary of the tide together with the sub-inertial oscillations described earlier. These oscillations were extrapolated to the open boundary from the Palmas Island tidal gauge using the methodology describe bellow. This sub-inertial variability of the water level was added linearly to the tide.

3.3. *Sub-inertial oscillations extrapolation*

The geostrophic balance was the starting hypothesis to extrapolate the sub-inertial oscillations form the tidal gauge of Palmas Island to the open boundary. The ADCP measurements (for a period of several months) show the reasonability of assuming that pressure is manly barotropic:

$$-g\frac{\partial \eta}{\partial y} = fu \qquad (2)$$

where η is the water level, y the cross shore direction (positive shore-ocean), f the coriolis frequency and u the velocity along shore. A typical solution of (2) is:

$$\eta(y) = \eta(0)e^{-\frac{f}{c}y} \qquad (3)$$

where c is the celerity of the sub-inertial perturbation. The relation c/f is the length scale associated with this perturbation. In this case the solution of the velocity along shore is:

$$u(y) = \frac{g}{c}\eta(y) \qquad (4)$$

Castro and Lee (1995) present a value of approximately 10 m/s for c for the study area of this work. Now, analyzing the ADCP and the tidal gauge data it is possible to verify that a strong correlation exists between the measured water level and the along shore velocity component, averaged in depth. This correlation is even clearer when all the variability with time scales lower than 4 days is filtered out (Figure 5). This last correlation is equal to 0.77.

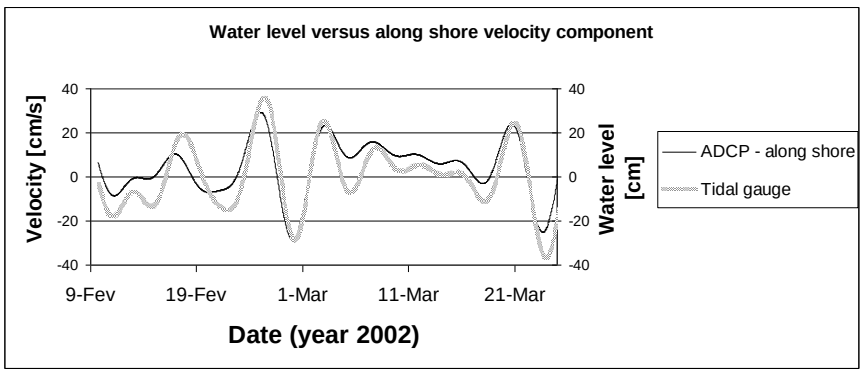

Figure 5– Water level measured in Palmas Island versus the along shore velocity component (variability below 4 days was filtered)

The expression resulting from the linear regression between the water level and the along shore velocity is:

$$u = 0.9\eta + 6 \qquad (5)$$

For velocities of the order of 20 cm/s it's reasonable to assume in the analyzed data set:

$$u \approx \frac{g}{10}\eta \qquad (6)$$

The data confirmed the geostrophic hypothesis and the celerity presented by Castro and Lee (1995). Expression (3) allows the extrapolation of the tidal gauge of Palmas Island in the cross shore direction. Now it is necessary to find a relation for the x direction (along shore). A first relation can be obtained if one considers that the sub-inertial oscillations are propagated as linear waves along the coast:

$$\frac{\partial \eta}{\partial t} + c\frac{\partial \eta}{\partial x} = 0 \qquad (7)$$

Another relation can be obtained from the forces balance:

$$\frac{\partial u}{\partial t} + g\frac{\partial \eta}{\partial x} = \frac{\tau_W}{\rho H} - \frac{C_D u}{H}\sqrt{u^2 + v^2} \qquad (8)$$

where τ_W is the wind shear stress, ρ is the water density, H the water column length and C_D the bottom drag coefficient. An order of magnitude analysis, based in the field data, compared the first left term and the two right terms. In this analysis it was possible to conclude that the bottom shear stress was the most important and therefore relation (8) can be simplified (9). Both relations (7) and (9) were tested in the hydrodynamic model validation process.

$$g\frac{\partial \eta}{\partial x} = -\frac{C_D u}{H}\sqrt{u^2 + v^2} \qquad (9)$$

3.4. *Sediment transport in the water column*

The lagrangian transport model is detailed in Miranda et al. (1999). This model uses a particle tracking approach, where a particle represents a water mass whose trajectory is tracked for a better understanding of local transport mechanisms. In this model the basic properties of used particles are their spatial co-ordinates and origin. In this work, other properties were associated with each particle like mass of sediment, particle volume, settling velocity, mixing length, and random velocity.

This type of model does not present numerical diffusion problems due to the calculation of advective transport. In general, diffusion is computed by adding a random component (turbulent velocity) to the mean velocity calculated by the hydrodynamic model. The effect of eddies over the particles depend on the ratio between the size of the eddy's and the size of the particles. Eddies larger than the particle cause a random movement of the particle. Eddies

smaller than the particle cause entrainment of matter into the particle increasing its mass and volume. The random movement is calculated following the procedure of Allen (1982). The random displacement is calculated using the mixing length and the standard deviation of the turbulent velocity component, as given by the turbulence closure of the hydrodynamic model.

3.5. *Bottom interface*

The methodology used in the MOHID system to compute the bottom interface processes of fine sediments is described in Cancino and Neves (1998) for a eulerian referential. The erosion algorithm used is based on the classical approach of Partheniades (1965). Erosion occurs when the ambient shear stress exceeds the threshold of erosion. In the lagrangian transport model, instead of erosion flux the probability of each particle deposited being eroded in a time step (Δt) is computed:

$$P_E = \min\left(1, \frac{E\Delta t}{M_A}\right) \text{ for } \tau > \tau_E \quad ; \quad P_E = 0 \text{ for } \tau < \tau_E \qquad (10)$$

where τ is the bed shear stress, τ_E is a critical shear stress for erosion and E is the erosion rate (kg $m^{-2}s^{-1}$). P_E is the probability of a particle being eroded, M_A the mass of sediment available to be eroded per square meter in the cell where the particle is deposited.

The algorithm used for estimating the sediment flux is the one proposed by Odd and Owen (1972). The algorithm is based on the assumption that a particle reaching the bottom has a probability of remaining there that varies between 0 and 1 as the bottom shear stress varies between its upper limit for deposition and zero, respectively (11).

$$P_D = \left(\frac{\tau_D - \tau}{\tau_D}\right) \text{ for } \tau < \tau_D \quad ; \quad P_D = 0 \text{ for } \tau > \tau_D \qquad (11)$$

where τ_D is a critical shear stress for deposition and P_D is the probability of a particle being deposited.

4. Results and Discussion

In a first phase, the hydrodynamic model was validated comparing the model results with the tidal gauge and the ADCP data for the period between February 23 and March 5, 2002. Two formulations to extrapolate the sub-inertial oscillations for the open boundary were tested. After the hydrodynamic model validation, the lagrangian sediment transport model presented earlier was ran

for several scenarios. The aim of these runs was to identify the area of influence of resuspended sediments, previously disposed in the bottom.

4.1. *Hydrodynamic model validation*

In the hydrodynamic validation process, special care was given to the imposition of the sub-inertial oscillations in the open boundary. In a first run, no sub-inertial oscillations were considered in the open boundary (Run 1). The goal of this run was to illustrate the importance of these perturbations in the final solution (Figure 6). Two more runs were made where Eq. (4) was used to extrapolate, in the cross shore direction, the sub-inertial oscillations measured in the Palmas Island tidal gauge to the open boundary. In the first run, Eq. (7) was used to extrapolate in the along shore direction the sub-inertial perturbations (Run 2). In the other run, the along shore extrapolation was done using (9) (Run 3). After analyzing the results, it is very clear that a coastal model to reproduce the coastal currents in the studied area must consider the sub-inertial oscillations described in this work. This is especially important for the along shore component (Figure 6). This methodology of using the sub-inertial oscillations in the open boundary very clearly improved the hydrodynamic results. When Eq. (9) is used to extrapolate the sub-inertial oscillations along shore, the model reproduces better the observed data than when Eq. (7)is used.

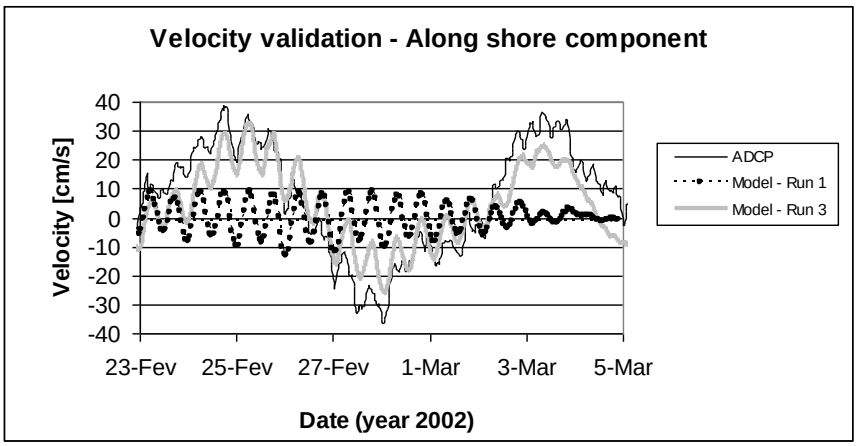

Figure 6 – Model results of along shore velocity component compared with ADCP data.

It was possible to improve the hydrodynamic results but some differences between the model and the observed data persist, especially in the along shore velocity component. The used methodology is very simplified because the sub-

inertial perturbation along the entire open boundary was estimated from only one tidal gauge.

A more realistic methodology, from the physics point of view, would be to explicitly simulate these sub-inertial oscillations. A possible methodology would be to simulate the entire East coast of South-America with a 2D hydrodynamic model coupled with an atmospheric model. This model should be able to reproduce the atmospheric perturbations that trigger the sub-inertial oscillations. Probably, it would be necessary in a future phase to run a 3D model and try to understand how Brazil current can influence the solution. This methodology is only possible to be implemented in the frame work of a large scientific project.

4.2. *Area of influence of discharge sites*

The quality of the hydrodynamic validation is sufficient to go on to the next step: the identification of the areas of influence of several disposal sites. The location of the disposal sites tested is represented in Figure 7. In the past, the dredged material was discharged in area 6 but now the discharge area is the 0 one.

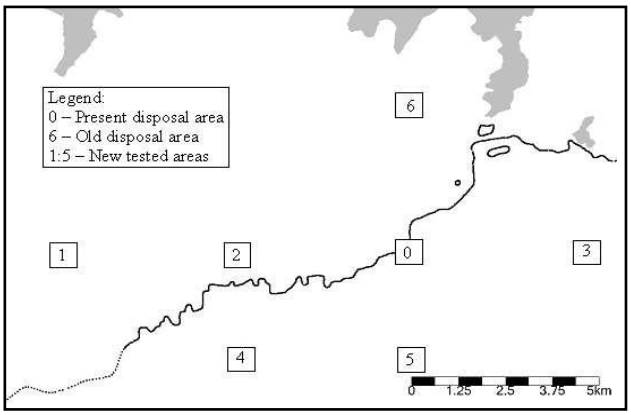

Figure 7 – Location of the disposal sites tested.

The lagrangian sediment transport model was used to follow the sediments when they were resuspended from the discharge area. The processes simulated were the horizontal transport induced by currents, erosion and sedimentation, settling and also the turbulent transport.

Due to the lack of data describing the dredge fine sediments properties was used typical values fiend in the literature (Mehta, 1988 and Houwing, 1999). The settling velocity was assumed equal to 0.1 mm/s. Two values of critical

shear stress for erosion were tested, 0.25 and 0.4 Pa. The critical shear stress for sedimentation was considered equal to 0.2 Pa and the erosion rate equal to 0.05 g/m2/s. In terms of turbulent transport, a standard deviation of the horizontal turbulent velocity equal to 10% of the current intensity was assumed. For the horizontal mixing length, a value of 2 times the spatial step was assumed. The vertical mixing length and the standard deviation of the turbulent velocity were estimated from a logarithmic profile (Allen 1982).

For the initial condition it was assumed that all particles (sediments) were deposited in each discharge area. The simulations had the main goal of following the trajectory of the sediments in two situations of currents intensification (westerly and easterly).

The results for the westerly current intensification scenario show a tendency for the resuspended sediments from the old discharge to enter again in the estuary (Figure 8). In the easterly current intensification scenario, the sediments resuspended from the old area had the tendency to settle along the shoreline. This was observed in the past and was the main reason why the disposal area was moved from area 6 to area 0 (Figure 7). Other disposal areas differ in the distance of the dispersion area perpendicular to the coast.

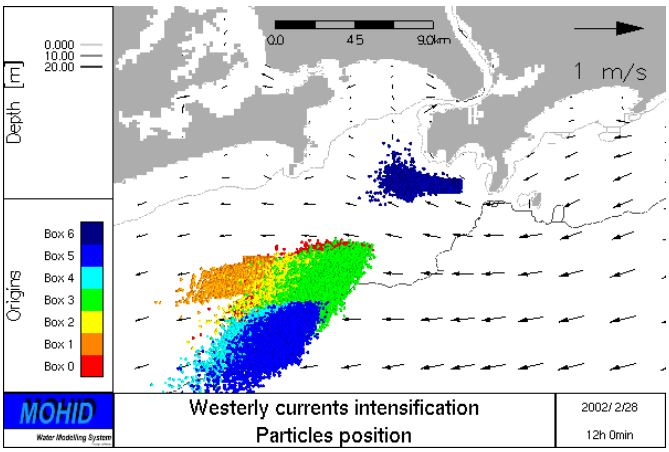

Figure 8 – Location of the particles position after one event of easterly current intensification.

References

Allen, C. M., 1982. Numerical simulation of contaminant dispersion in estuary flows. Proc. R. Soc. London. A 381, 179-194.

Camargo, R., Harari, J. and Caruzzo, A., 1999. Basic Statistics of Storm Surges Over The South Western Atlantic. Afro-America Gloss News, V 3 (2).

Cancino, L. and Neves, R.J.J, 1998. Hydrodynamic and sediment suspension modelling in estuarine systems. Part I: description of the numerical models. Journal of Marine Systems 22, 105-116.

Castro, B. M. and Lee, T. N., 1995. Wind-forced sea level variability on the southeast Brazilian shelf. J.Geophys.Res., V 100 (C8), pp 16045-16056.

Coelho, H.S., Neves, R. J. J., White, M., Leitão, P.C. and Santos, A. J., 2002. A model for ocean circulation on the Iberian coast. Journal of Marine Systems 32, 153– 179.

Houwing, E.J., 1999. Determination of the critical erosion threshold of cohesive sediments on intertidal mudflats along the Dutch Wadden Sea coast. Estuarine, Coastal, and Shelf Science 49, 545 - 555.

Marchesiello, P., J. C. McWilliams and A. Shchepetkin, 2001. Open boundary conditions for long-term integration of regional oceanic models. Ocean Modelling 3, 1-20.

Martins, F., R. Neves, P. Leitão and A. Silva, 2001. 3D modeling in the Sado estuary using a new generic coordinate approach. Oceanologica Acta, 24:S51-S62.

Mehta, A.J., 1988. Laboratory studies of cohesive sediment deposition and erosion. In: Dronker, J., and van Leussen, W. (eds.). Physical Processes in Estuaries. Springer, Berlin, pp. 427 - 445.

Miranda, R., Neves, R., Coelho, H., Martins, H., Leitão, P. C. and Santos, A., 1999. Transport and mixing simulation along the continental shelf edge using a lagrangian approach, Boletín. Instituto Español de Oceanografía 15 (1-4), 39-60.

Odd, N.V.M. and Owen, M.W., 1972. A two-layer model of mud transport in the Thames estuary. In: Proceedings. Institution of Civil Engineers, London, pp. 195–202.

Oey, L. and P. Chen, 1992. A Nested-Grid Ocean Model: With Application to the Simulation of Meanders and Eddies in the Norwegian Coastal Current. J. Geophys. Res., 97, 20,063-20,086.

Partheniades, E., 1965. Erosion and deposition of cohesive soils. J. Hydr. Div., ASCE 91 HY1 , 105–139.

Tartinville, B., E. Deleersnijder, P. Lazure, R. Proctor, K. G. Ruddick and R. E. Uittenbogaard, 1998. A coastal ocean model intercomparison study for a three-dimensional idealised test case. Applied Mathematical Modelling, 22(3): 165-182.

KEYWORDS – ICCE 2004

HYDRODYNAMICS AND TRANSPORT IN THE COASTAL ZONE OF SÃO PAULO – BRAZIL

Paulo C. Leitão, José C. Leitão, Ramiro Neves, Gilberto Berzin and Adélio J. R. Silva

Abstract 284

Harbor
Dredging
Disposal
Modeling
Tide
Sub-inertial oscillations
Fine sediment
Particle tracking